A NOVEL DOA-BASED BEAMFORMING ALGORITHM WITH BROAD NULLS

M. Taferner, A. Kuchar*, M.C. Lang*, M. Tangemann**, C. Hoek***

* Institut für Nachrichtentechnik und Hochfrequenztechnik
Technische Universität Wien, Vienna
Gusshausstrasse 25/389, A-1040 Wien, Austria
Tel: (+431) 58 801/389 84 Fax: (+431) 58801/38999
email: Manfred.Taferner@nt.tuwien.ac.at

** Alcatel Corporate Research Center Stuttgart
D – 70430 Stuttgart, Germany

Abstract: We present a novel direction–of–arrival (DOA) based beamforming algorithm and compare its BER performance in a real–time smart antenna processor system with other beamforming methods. To combat multipath propagation with significant angular spread (several degrees) in mobile communication systems, the algorithm places broad nulls as well as maintaining a low sidelobe level.

Our algorithm provides flexible parameter adjustment (sidelobe level, main beam width, null depth and null width) together with very low computational effort. The run–time of the algorithm is below 60μs on a 500MHz DEC–Alpha processor for an 8 element array.

When tested with synthetic data with large angular spread, the novel beamformer achieves better signal–to–noise and interference ratio (SNIR) than other state–of-the–art algorithms. The BER performance of the novel beamformer does not degrade as long as the DOA estimation error is smaller than one degree.

1. INTRODUCTION

Adaptive antennas will be used in mobile communication systems to enhance coverage, reduce co–channel interference, and increase capacity [1, 2, 3]. In an FDD system like GSM and UMTS W–CDMA, the small–scale fading is different in uplink and downlink. All beamforming methods that rely on an estimate of the instantaneous channel characteristics are therefore not applicable in the downlink. The presented beamforming algorithm is suitable for uplink and downlink since it is based on the DOAs estimated in uplink. It relies on the *averaged* azimuthal power spectrum being constant in uplink and in downlink. From the DOAs a beamforming algorithm extracts a weight vector that maximizes the gain into the direction of a user while nulling out the interferers, thus maximizing SNIR.

In this paper we present a novel beamforming algorithm. The algorithm is capable of placing broad nulls while maintaining a low sidelobe level. A broad null is important, because in mobile radio channels significant angular spreads are common [4].

We present a thorough evaluation of the beamforming algorithm by comparing the SNIR and BER performance of the antenna processor in a synthetic channel with that of other state–of–the–art beamformers. Integration of the beamformer into a real–time smart antenna processor, called **A^{3}P**, is presented in [5, 6].

2. SYSTEM MODEL

The system model is shown in Fig. 1. The array processor estimates the DOAs from the uniform linear antenna array output samples $\mathbf{X}$ ($M \times N$), where M is the number of antenna elements and N denotes the number of samples in one burst. After classification of DOAs into a single user DOA[1], Θ_U, and interferer DOAs, $\Theta_{I,i}, i = 1 \ldots D_I$, and subsequent DOA tracking, the beamforming algorithm extracts the beamforming weight vector, $\mathbf{w}$ ($M \times 1$), to optimize SNIR. With the calculated weight vector, $\mathbf{w}$, we extract the estimated user signal, $\hat{\mathbf{s}}$ ($1 \times N$),

$$\hat{\mathbf{s}} = \mathbf{w}^H \mathbf{X}. \tag{1}$$

3. BEAMFORMING ALGORITHMS

We present a new beamforming algorithm, **SmearR**, that is able to place broad nulls and provides flexible parameter setting.

For comparison purpose we refer to two state–of–the–art beamforming algorithms.

[1] The system is able to exploit more than a single user–DOA (angular diversity) but in this paper we asses only a single user DOA for simplicity.

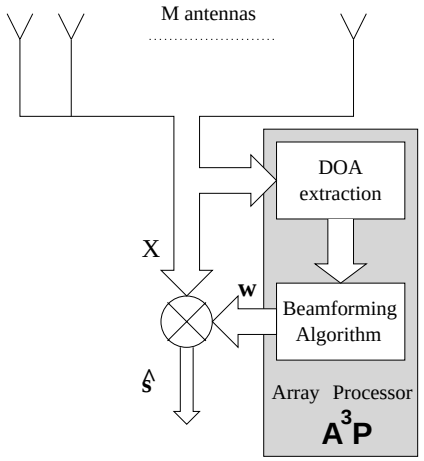

Figure 1: Used system model for signal separation with smart antennas.

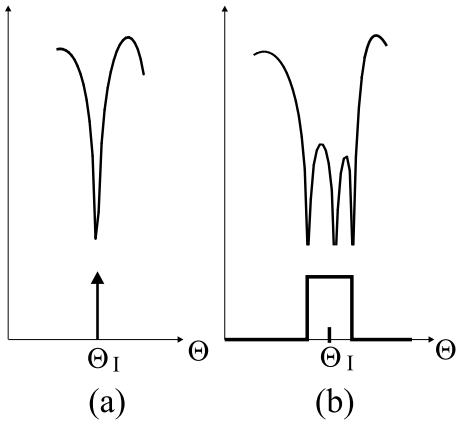

Figure 2: Portion of the antenna pattern (above) and wavenumber–frequency spectrum (below) a null: (a) Dirac–shaped wavenumber–frequency spectrum; (b) smeared wavenumber–frequency spectrum.

3.1. Beamforming algorithm SmearR

We modified Capon's beamformer, where the weight vector $\mathbf{w}$ can be obtained from [7],

$$\mathbf{w} = \boldsymbol{R}^{-1} \cdot \boldsymbol{a}_{\Theta_U} \,. \tag{2}$$

Here $\boldsymbol{a}_\Theta = [1, e^{-jkd\sin(\Theta)}, \ldots, e^{-j(M-1)kd\sin(\Theta)}]^T$ denotes the steering vector of the user DOA, Θ_U, for a uniform linear array[2]. d is the distance between antenna elements and $k = 2\pi/\lambda$ the wave number.

Instead of using the well known estimate of the spatial covariance matrix, $\boldsymbol{R} = \mathbf{X}\mathbf{X}^H$, we base $\boldsymbol{R}$ on the estimated DOAs:

$$\boldsymbol{R} = \boldsymbol{A}\boldsymbol{A}^H + \sigma^2 \boldsymbol{I} \,, \tag{3}$$

where

$$\boldsymbol{A} = [\boldsymbol{a}_{\Theta_U}, \boldsymbol{a}_{\Theta_{I,1}}, \ldots, \boldsymbol{a}_{\Theta_{I,D_I}}] \tag{4}$$

is the steering matrix of the estimated user and interferer DOAs, σ^2 is the noise power and $\boldsymbol{I}$ is the identity matrix. Adding a noise term is necessary to avoid a singular covariance matrix. However, Eq. 3 corresponds to a Dirac–shaped wavenumber–frequency spectrum[3] for the interferer DOAs.

The basic idea of **SmearR** is to *avoid* a Dirac–shaped wavenumber–frequency spectrum for the interferers. Instead we use a wavenumber–frequency spectrum for each interferer that is broadened but in principle arbitrarily shaped, to achieve broad nulls in the antenna pattern (Fig. 2). Thus the covariance matrix is *not* computed from the steering vectors of the interfering signals, $\boldsymbol{a}_{\Theta_{I,i}}$, but from 'smeared' versions of the interferer steering vectors,

$$\tilde{\boldsymbol{a}}_{\Theta_{I,i}} = \boldsymbol{a}_{\Theta_{I,i}} \odot \boldsymbol{v}_{\Theta_{I,i}} \,, \quad 1 \le i \le D_I \,. \tag{5}$$

[2]However, the algorithm is not limited to uniform linear arrays.

[3]The wavenumber–frequency spectrum is defined as the discrete Fourier transform of the array response [11]. In the special case of a plane wave incident on a uniform linear array the wavenumber–frequency spectrum consists of a Dirac impulse, and the corresponding array response is the steering vector.

$\odot$ denotes elementwise multiplication. $\boldsymbol{v}_{\Theta_{I,i}}$ is the inverse Fourier transform of each interferer wavenumber–frequency spectrum sampled at the antenna elements, in our case

$$\boldsymbol{v}_{\Theta_{I,i}} = ND_i \left[1, \frac{sin(\delta_i)}{\delta_i}, \ldots, \frac{sin((M-1)\delta_i)}{(M-1)\delta_i}\right] \,, \tag{6}$$

where $\delta_i = NW/2 \cdot \pi\cos(\Theta_{I,i})$ denotes the half of the desired normalized null width, NW, and ND_i an interferer dependent weighting constant that determines the null depth. Equation 6 and Fig 2,b show an example for a rectangular shaped wavenumber–frequency spectrum in beamspace, but any arbitrarily shaped wavenumber–frequency spectrum can be applied. This 'smeared' wavenumber–frequency spectrum guarantees the broad nulls in the pattern.

To obtain an adjustable sidelobe level we modify the steering vector of the user DOA, $\boldsymbol{a}_{\Theta_U}$, with a noise term. In beamspace the noise term has a constant wavenumber–frequency spectrum outside the main beam and is zero in the main beam region with a width of BW:

$$\tilde{\boldsymbol{a}}_{\Theta_U} = \boldsymbol{a}_{\Theta_U} \odot \boldsymbol{v}_N \,, \tag{7}$$

where the shaping vector,

$$\boldsymbol{v}_N = \left[1, \frac{2sin(BW'/2)}{2\pi - BW'}, \ldots, \frac{2sin((M-1)BW'/2)}{(M-1)(2\pi - BW')}\right] \,, \tag{8}$$

corresponds to the shape of the wavenumber–frequency noise spectrum. Thus a large nominal beam width, BW, gives a low sidelobe level and vice versa. The actual beam width, BW', is given by $BW' = BW \cdot \pi\cos(\Theta_U)$.

Now a modified steering matrix,

$$\tilde{\boldsymbol{A}} = [\tilde{\boldsymbol{a}}_{\Theta_U}, \tilde{\boldsymbol{a}}_{\Theta_{I,1}}, \ldots, \tilde{\boldsymbol{a}}_{\Theta_{I,D_I}}], \tag{9}$$

and finally a modified spatial covariance matrix,

$$\tilde{\boldsymbol{R}} = \tilde{\boldsymbol{A}}\tilde{\boldsymbol{A}}^H \ , \tag{10}$$

can be computed and inserted in Eq. 2 to get the weight vector. Here the noise term $\sigma^2\boldsymbol{I}$ is not present because it is already included in $\tilde{\boldsymbol{a}}_{\Theta_U}$.

Because the modified angular covariance matrix, $\tilde{\boldsymbol{R}}$, has Toeplitz structure, the complex–valued Levinson–algorithm [8] can be used for very efficient calculation of $\mathbf{w}$.

An advantage of the described algorithm is the simple adjustment of the required pattern constraints by directly setting the parameters null width, NW, beam width, BW, and null depth, ND. The parameters can be set independently within wide limits, but, of course, are subject to physical constraints.

3.2. Chebychev pattern synthesis with broad nulls

For comparison we use a modified Chebychev beamformer with broad nulls.

The Chebychev pattern synthesis uses the Dolph–Chebychev pattern [9] with successive pattern cancellation.

To place broad nulls we use the pattern cancellation scheme from [10]. Here cancellation patterns are subtracted for each interferer DOA from the original Dolph–Chebychev pattern to achieve broad nulls.

3.3. Pseudo inverse beamforming

A simple approach to place sharp nulls into the directions of the interferers, while maintaining a constant gain in user direction is the Moore–Penrose pseudo inverse [11]:

$$\boldsymbol{W}^H = \boldsymbol{A}^\dagger \ , \tag{11}$$

where $\boldsymbol{A}$ is defined in Eq. 4.

The weight vector $\mathbf{w}$ is the first column vector of $\boldsymbol{W}$.

4. REAL–TIME ADAPTIVE ANTENNA ARRAY PROCESSOR

We developed a real–time adaptive antenna array processor **A³P** (Fig. 3) for a DCS 1800 base station. The **A³P** uses the calibrated digital baseband signal in the uplink to calculate the antenna weights for uplink and downlink beamforming. Processing is based on a DOA estimation (**DOAE**) which employs in our case Unitary ESPRIT [12]. A spatial pre-filter, the uplink beamformer (**ULBF**), and a user identification (**UID**) decide whether a DOA belongs to the user or to an interferer. The tracker (**DOAT**) averages the user DOAs and improves the reliability of the user DOAs. The final uplink post beamforming algorithm **ULpBF** puts a main beam into the tracked user direction, while placing deep broad nulls into the direction of the interferers.

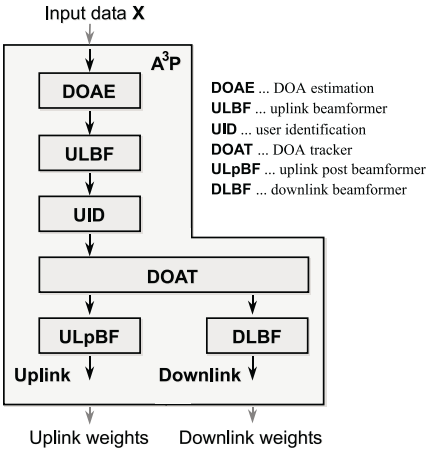

Figure 3: Adaptive antenna array processor **A³P**.

In the succeeding performance evaluation, each of the beamforming algorithms described in Section 3 is used in both **ULBF** and **ULpBF**. For a detailed discussion of **A³P** we refer to [5, 6].

5. PERFORMANCE EVALUATION

We assess the beamforming algorithms by investigating their influence on the **A³P**'s performance, i.e. on the mean SNIR improvement and on the raw bit–error–rate (BER).

We generate synthetic test data with our Geometry based Stochastic Channel Model, GSCM, [13]. The GSCM is based on local scatterers that are distributed around the mobile stations, thus leading to small-scale fading. A realization of the used channel configuration is shown in Fig. 4. The user is located at $+10°$ and a single interferer at $-20°$. The user transmits with a 5 dB lower mean power than the interferer. The number of antenna elements is $M = 8$.

In a first step we investigate the post beamformer **ULpBF**. At first we use the ideal DOAs instead of estimates because we focus on the influence of the beamforming algorithms . The angular spread has a significant effect on system performance. We simulated about 5000 GSM bursts with independent small–scale fading for various settings of the angular spread. In the GSCM the angular spread is defined as the second order moment of the angular power spectrum [14].

The mean input SNIR varies with the angular spread as a consequence of the channel model (Fig. 5). **SmearR** has the highest output SNIR regardless of the angular spread except for the pseudo inverse at the very small angular spread of $0.1°$. In the case of ideal DOAs, interference suppression of the algorithm that places sharp nulls is in principle unlimited. In our simulations the mean output SNIR is limited to 29 dB, which is the consequence of a finite mean input SNR of 20 dB and the maximum average SNR gain of $10\log M = 9.03$ dB for an 8–element array. While for **SmearR** the SNIR reaches up to the max-

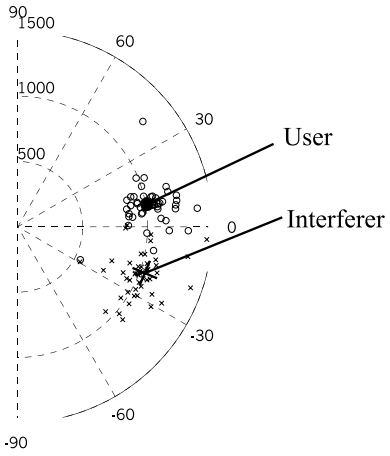

Figure 4: Realization of a GSCM scatterer distribution for an angular spread of 30°. The user mobile station is located at +10° and a single interferer at −20°. The small circles (crosses) symbolize the local scatterers for user (interferer). The distance between local scatterers and mobile stations has Gaussian distribution with a variance depending on the angular spread [14].

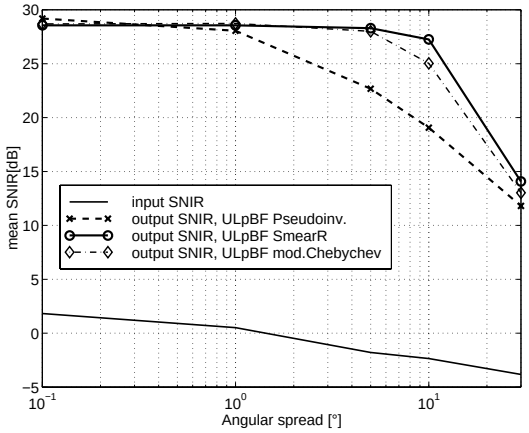

Figure 5: Influence of **ULpBF** algorithms on mean output SNIR. Note that the mean input SNIR decreases with increasing angular spread due to the channel properties. As **ULBF** we used the pseudo inverse and ideal DOAs. The mean input SNR is 20 dB throughout.

imum (noise–limited case, SNR=SNIR) nearly independently of the angular spread, the pseudo inverse is still interference limited for an angular spread larger than 1°.

The performance of **SmearR** starts to degrade only when the angular spread is larger than the null width (in our case $NW = 10°$). Using a larger setting of NW increases performance in such a scenario. But in general this might not be the case with a larger number of interferers.

SmearR has a BER that is up to an order of magnitude smaller (Fig. 6) compared to the pseudo inverse, and a factor of up to two smaller compared to the modified Chebychev algorithm. Because the mean input SNIR decreases with increasing angular spread (Fig. 5), the BER curves (Fig. 6) can only be compared for each angular spread setting individually.

In another simulation we added to the ideal DOA an Gaussian distributed estimation error. For the beamforming algorithms with broad nulls (**SmearR**, mod. Chebychev) the BER starts to degrade only for a standard deviation larger than one degree, while it degrades already for smaller estimation errors with the pseudo inverse (Fig. 7). Thus **SmearR** is considerably more robust against DOA estimation errors.

5.1. Computational complexity

Computational complexity of the beamforming algorithms depends on the number of interferer DOAs, i.e. the number of broad nulls.

We implemented all three algorithms in the real–time smart antenna processor **A^{3}P**. The results of the run–time measurements on a 500MHz DEC Alpha processor are shown in Tab. 1.

Algorithm	#Intf=1	#Intf=5
SmearR	40 μs	55 μs
modified Chebychev	42 μs	75 μs
pseudo inverse	66 μs	192 μs

Table 1: Run–time measurements of algorithms implemented in C–code on a 500MHz DEC Alpha processor.

The pseudo inverse algorithm more strongly depends on the number of interferer DOAs than the other algorithms. The **SmearR** and the modified Chebychev algorithm have almost equal run–times for one interferer DOA, but **SmearR** outperforms the modified Chebychev beamformer in the presence of more interferers. Thus **SmearR** is the most suitable beamforming algorithm for a real–time system.

6. SUMMARY AND CONCLUSION

We described a novel DOA–based beamforming algorithm. It places broad nulls into the direction of interferers. This increases the system–robustness in two ways:

- Interference suppression degrades less for large angular spreads.
- The system is more robust against DOA estimation errors.

The measured run–time for the proposed algorithm is below 60μs. This very low computational complexity comes together with a flexible parameter setting of sidelobe level, null depth and null width and makes

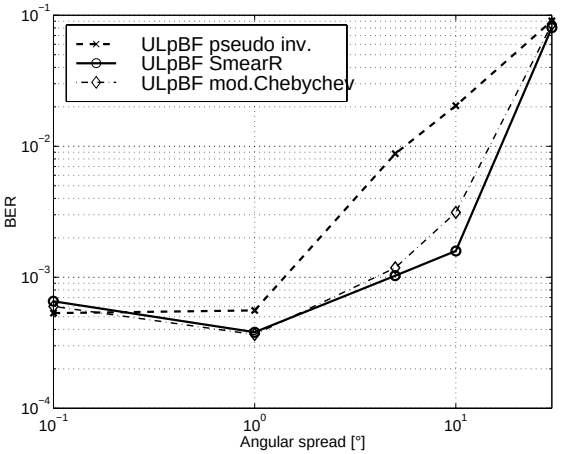

Figure 6: Influence of **ULpBF** algorithms on BER. We used the pseudo inverse as **ULBF**. Because the mean input SNIR decreases with increasing angular spread (Fig. 5) the BER curves can only be compared for each angular spread setting individually.

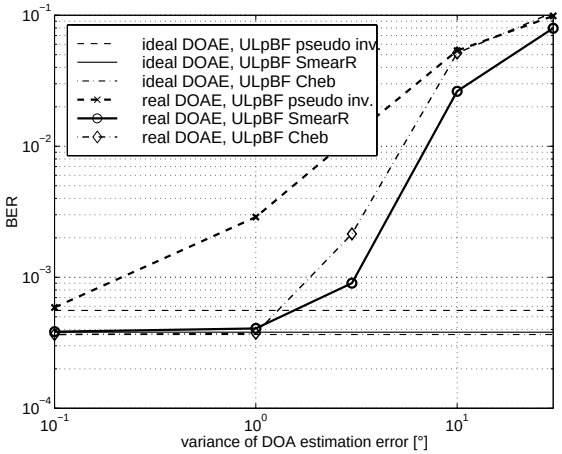

Figure 7: Influence of DOA estimation errors on BER. We used the pseudo inverse as **ULBF**. Because the mean input SNIR decreases with increasing angular spread (Fig. 5) the BER curves can only be compared for each DOA estimation error setting individually.

our algorithm excellently suitable for real–time smart antenna applications in mobile communication systems.

7. ACKNOWLEDGEMENT

We thank Prof. E. Bonek and A. F. Molisch for valuable discussions and comments on this work.

8. REFERENCES

[1] M. Tangemann, C. Hoek, R. Rheinschmitt, "Introducing Adaptive Array Antenna Concepts in Mobile Communications Systems", Proceedings RACE Mobile Telecommunications Workshop, Amsterdam, May 17–19, 1994, Volume 2, pp. 714–727.

[2] J. H. Winters, "Smart Antennas for Wireless Systems", IEEE Personal Communications Magazine, February 1998, pp. 23–27.

[3] Ryuji Kohno, "Spatial and Temporal Communication Theory using Adaptive Antenna Array", IEEE Personal Communications, February 1998, pp. 28-35.

[4] K.I. Pedersen, P.E. Mogensen, B.H. Fleury, "Power azimuth spectrum in outdoor environments", *Electronics Letters*, 28th August 1997, Vol.33, No.18, pp.1583-1584

[5] A. Kuchar, M. Taferner, M. Tangemann, C. Hoek, W. Rauscher, M. Strasser, G. Pospischil, and E. Bonek, "Real–time Smart Antenna Processing for GSM1800 Base Station", Vehicular Technology Conference VTC '99, Houston, May 16.-20. 1999.

[6] A. Kuchar, M. Taferner, M. Tangemann, C. Hoek, W. Rauscher., M. Strasser, G. Pospischil, and E. Bonek, "A Robust DOA-based Smart Antenna Processing for GSM Base Stations", IEEE Intern. Conference on Communications ICC '99, Vancouver, June 6.-10. 1999.

[7] J. Capon, R.J. Greenfield, and R.J. Kolker "Multidimensional maximum–likelihood processing of a large aperture seismic array", *Proc. IEEE*, 55, pp. 192-211, Feb. 1967.

[8] N. Levinson, "The Wiener RMS Criterion in Filter Design and Prediction," *J. Math. Phys.*, vol. 25, pp. 261-278, Jan. 1947.

[9] C.L. Dolph: "A Current Distribution for Broadside Arrays Which Optimizes the Relationship Between Beamwidth and Sidelobe Level" *Proc. IRE*, Vol. 34, June 1946, pp. 335-345.

[10] H. Steyskal, R.A. Shore, R.L. Haupt: "Methods for Null Control and Their Effects on the Radiation Pattern", *IEEE Trans. on Antennas and Propagation*, Vol. AP–34, No. 3, March 1986.

[11] Don H. Johnson, and Dan E. Dudgeon, "Array Signal Processing, Concepts and Techniques", Prentice–Hall Signal Processing Series, 1991.

[12] M. Haardt and J. A. Nossek, "Unitary ESPRIT: How to Obtain Increased Estimation Accuracy with a Reduced Computational Burden", IEEE Transactions on Signal Processing, Vol. 43, No. 5, pp. 1232–1242, May 1995.

[13] J. Fuhl, A.F. Molisch, and E. Bonek, "Unified channel model for mobile radio systems with smart antennas", IEE Proc.-Radar, Sonar Navigation, Vol. 145, No. 1, February 1998.

[14] Laurila J., Molisch A.F., Bonek, E. "Influence of the scatterer distribution on power delay profiles and azimuthal power spectra of mobile radio channels", IEEE International Symposium on Spread Spectrum Techniques and Applications (ISSSTA '98), Sun City, South Africa, September 2-4, 1998, p. 267-271.